DESY 06-004
Edinburgh 2006/02
Liverpool LTH 686
February 2006

Determining the strange quark mass for 2-flavour QCD*

M. Göckeler[a], R. Horsley[b], A. C. Irving[c], D. Pleiter[d], P. E. L. Rakow[c], G. Schierholz[d,e], H. Stüben[f] and J. M. Zanotti[b]
– *QCDSF–UKQCD* Collaboration –

[a]Institut für Theoretische Physik, Universität Regensburg, D-93040 Regensburg, Germany

[b]School of Physics, University of Edinburgh, Edinburgh EH9 3JZ, UK

[c]Department of Mathematical Sciences, University of Liverpool, Liverpool L69 3BX, UK

[d]John von Neumann Institute NIC / DESY Zeuthen, D-15738 Zeuthen, Germany

[e]Deutsches Elektronen-Synchrotron DESY, D-22603 Hamburg, Germany

[f]Konrad-Zuse-Zentrum für Informationstechnik Berlin, D-14195 Berlin, Germany

Using the $O(a)$ Symanzik improved action an estimate is given for the strange quark mass for unquenched ($n_f = 2$) QCD. The determination is via the axial Ward identity (AWI) and includes a non-perturbative evaluation of the renormalisation constant. Numerical results have been obtained at several lattice spacings, enabling the continuum limit to be taken. Our results indicate a value for the strange quark mass (in the $\overline{MS}$-scheme at a scale of 2 GeV) in the range 100 – 130 MeV. A comparison is also made with other recent lattice determinations of the strange quark mass using dynamical sea quarks.

1. INTRODUCTION

Lattice methods allow, in principle, the complete 'ab initio' calculation of the fundamental parameters of QCD, such as quark masses. However quarks are not directly observable, being confined in hadrons and are thus not asymptotic states. So to determine their mass necessitates the use of a non-perturbative approach – such as lattice QCD or QCD sum rules. In this brief article, we report on our recent results for the strange quark mass for 2-flavour QCD in the $\overline{MS}$-scheme at a scale of 2 GeV, $m_s^{\overline{MS}}(2\,\mathrm{GeV})$ (further details can be found in [1]).

The present phenomenological status is summarised by the Particle Data Group in [2] giving an estimate for the strange quark mass of $80\,\mathrm{MeV} < m_s^{\overline{MS}}(2\,\mathrm{GeV}) < 130\,\mathrm{MeV}$. This is a large band, and it is be hoped that lattice computations will reduce this significantly in the coming years.

*Talk given by R. Horsley at the Workshop on Computational Hadron Physics, (Nicosia, Cyprus, September '05).

2. RENORMALISATION GROUP INVARIANTS

Being confined, the mass of the quark, $m_q^{\mathcal{S}}(M)$, needs to be defined by giving a scheme, $\mathcal{S}$ and scale M,

$$m_q^{\mathcal{S}}(M) = Z_m^{\mathcal{S}}(M) m_q^{BARE}\,, \qquad (1)$$

and thus we need to find both the bare quark mass and the renormalisation constant. An added complication is that the $\overline{MS}$-scheme is a perturbative scheme, while more natural schemes which allow a non-perturbative definition of the renormalisation constants have to be used. It is thus convenient to first define a (non-unique) renormalisation group invariant (RGI) object, which is both scale and scheme independent by

$$m_q^{RGI} \equiv \Delta Z_m^{\mathcal{S}}(M) m^{\mathcal{S}}(M) \equiv Z_m^{RGI} m_q^{BARE}\,, \qquad (2)$$

where we have

$$[\Delta Z_m^{\mathcal{S}}(M)]^{-1} \equiv \left[2b_0 g^{\mathcal{S}}(M)^2\right]^{-\frac{d_{m0}}{2b_0}} \times$$

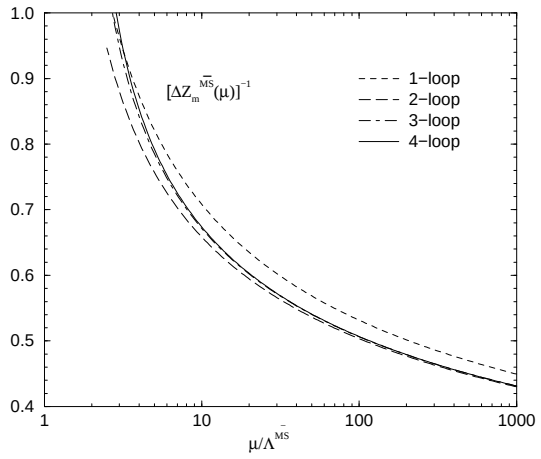

Figure 1. One-, two-, three- and four-loop results for $[\Delta Z_m^{\overline{MS}}(\mu)]^{-1}$ in units of $\Lambda^{\overline{MS}}$.

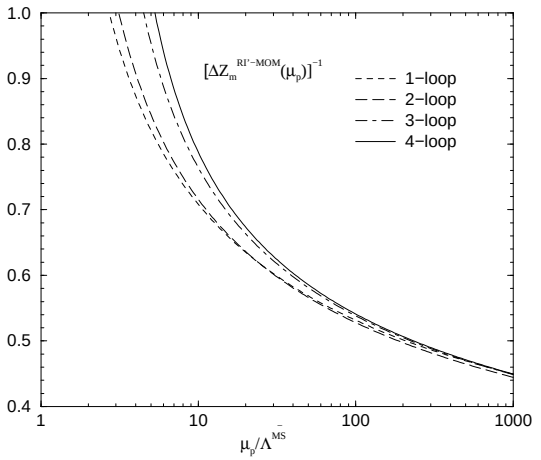

Figure 2. One-, two-, three- and four-loop results for $[\Delta Z_m^{RI'-MOM}(\mu_p)]^{-1}$ in units of $\Lambda^{\overline{MS}}$.

$$\exp\left\{\int_0^{g^{\mathcal{S}}(M)} d\xi \left[\frac{\gamma_m^{\mathcal{S}}(\xi)}{\beta^{\mathcal{S}}(\xi)} + \frac{d_{m0}}{b_0\xi}\right]\right\}. \qquad (3)$$

The $\beta^{\mathcal{S}}$ and $\gamma_m^{\mathcal{S}}$ functions (with leading coefficients $-b_0$, d_{m0} respectively) are known perturbatively up to a certain order[1]. In the $\overline{MS}$ scheme the first four coefficients are known, [3,4], and this is also true for the RI′-MOM scheme [5,6] (which is a suitable scheme for both perturbative and non-perturbative, NP, applications, see section 4). Note that in the RI′-MOM scheme we also choose to expand the $\beta^{\mathcal{S}}$ and $\gamma_m^{\mathcal{S}}$ functions in terms of $g^{\overline{MS}}$, [6]; other choices, of course, are also possible.

In Figs. 1 and 2 we show the results of solving eq. (3) as a function of the scale $M \equiv \mu$ and $M \equiv \mu_p$ for both the $\overline{MS}$ and RI′-MOM schemes respectively. We hope to use these (perturbative) results in a region where perturbation theory has converged. 2 GeV corresponds to $\mu/\Lambda^{\overline{MS}} \sim 8$, where it would appear that the expansion for the $\overline{MS}$-scheme has converged; for the RI′-MOM scheme using a higher scale is safer (which is chosen in practice). However, when the RGI quantity has been determined we can then easily change from one scheme to another. Of course these scales are in units of $\Lambda^{\overline{MS}}$ which is awkward to use: the standard 'unit' nowadays is the force scale r_0. To convert to this unit, we use the result for $r_0\Lambda^{\overline{MS}}$ as given in [7]. Of course, we must also give the physical scale. A popular choice is $r_0 = 0.5\,\text{fm}$, but there is some variation in possible values, see section 6.

[1] Analgous definitions also hold for other operators, see section 4.

3. CHIRAL PERTURBATION THEORY

We have generated results for $n_f = 2$ degenerate sea quarks, together with a range of valence quark masses. Chiral perturbation theory, χPT, has been developed for this case, [8,9]. We have manipulated the structural form of this equation to give an ansatz of the form

$$\begin{aligned} r_0 m_s^{RGI} = \\ & c_a^{RGI}\left[(r_0 m_{K^+})^2 + (r_0 m_{K^0})^2 - (r_0 m_{\pi^+})^2\right] + \\ & (c_b^{RGI} - c_d^{RGI})\left[(r_0 m_{K^+})^2 + (r_0 m_{K^0})^2\right] \times \\ & \qquad (r_0 m_{\pi^+})^2 + \\ & \tfrac{1}{2}(c_c^{RGI} + c_d^{RGI})\left[(r_0 m_{K^+})^2 + (r_0 m_{K^0})^2\right]^2 - \\ & (c_b^{RGI} + c_c^{RGI})(r_0 m_{\pi^+})^4 - \\ & c_d^{RGI}\left[(r_0 m_{K^+})^2 + (r_0 m_{K^0})^2\right] \times \\ & \quad \left[(r_0 m_{K^+})^2 + (r_0 m_{K^0})^2 - (r_0 m_{\pi^+})^2\right] \times \\ & \quad \ln\left((r_0 m_{K^+})^2 + (r_0 m_{K^0})^2 - (r_0 m_{\pi^+})^2\right) + \\ & c_d^{RGI}(r_0 m_{\pi^+})^4 \ln(r_0 m_{\pi^+})^2\,, \end{aligned} \qquad (4)$$

where

$$\frac{r_0 m_q^{RGI}}{(r_0 m_{ps})^2} = c_a^{RGI} + c_b^{RGI}(r_0 m_{ps}^S)^2 + c_c^{RGI}(r_0 m_{ps})^2 + c_d^{RGI}\left((r_0 m_{ps}^S)^2 - 2(r_0 m_{ps})^2\right)\ln(r_0 m_{ps})^2 \,. \quad (5)$$

m_{ps}, m_{ps}^S are the valence and sea pseudoscalar masses respectively (both using mass degenerate quarks). The first term is the leading order, LO, result in χPT while the remaining terms come from the next non-leading order, NLO, in χPT. Thus we see from eq. (5) that to NLO, we can first determine c_a^{RGI} and c_i^{RGI}, $i = b, c, d$ using pseudoscalar mass *degenerate* quarks and then simply substitute them in eq. (4).

4. THE LATTICE APPROACH

Approaches to determining the quark mass on the lattice are to use the vector Ward identity, VWI (see e.g. [10]), where the bare quark mass is given in terms of the hopping parameter by[2]

$$m_q = \frac{1}{2a}\left(\frac{1}{\kappa_q} - \frac{1}{\kappa_{qc}^S}\right) , \quad (6)$$

or the axial Ward identity, AWI, which is the approach employed here. Imposing the AWI on the lattice for mass degenerate quarks, we have

$$\partial_\mu \mathcal{A}_\mu = 2\widetilde{m}_q \mathcal{P} + O(a^2) \,, \quad (7)$$

and $\mathcal{A}$ and $\mathcal{P}$ are the $O(a)$ improved[3] unrenormalised axial current and pseudoscalar density respectively and $\widetilde{m}_q$ is the AWI quark mass. So by forming two-point correlation functions with $\mathcal{P}$ in the usual way, this bare quark mass can be determined

$$a\widetilde{m}_q \overset{t\gg 0}{=} \frac{\langle \partial_4^{LAT} \mathcal{A}_4(t)\mathcal{P}(0)\rangle}{2\langle \mathcal{P}(t)\mathcal{P}(0)\rangle} \,. \quad (8)$$

[2]This is valid for both valence and sea quarks. κ_{qc}^S is defined for fixed β by the vanishing of the pseudoscalar mass, i.e. $m_{ps}(\kappa_{qc}^S, \kappa_{qc}^S) = 0$. κ_{qc}^S has been determined in [10].

[3]The improvement term to the axial current, $\partial_\mu P$ together with improvement coefficient c_A, [11] has been included. The mass improvement terms, together with their associated difference in improvement coefficients, b_A, b_P appear to be small and have been ignored here.

We have found results for four β-values: 5.20, 5.25, 5.29, 5.40, each with several (three or more) sea quark masses and a variety of valence quark masses, [1].

Furthermore upon renormalisation we have

$$\mathcal{A}_\mu^{\mathcal{R}} = Z_A \mathcal{A}_\mu \,, \qquad \mathcal{P}^{\mathcal{S}}(M) = Z_P^{\mathcal{S}}(M)\mathcal{P} \,, \quad (9)$$

giving from eqs. (2) and (7)

$$Z_{\tilde{m}}^{RGI} = \Delta Z_{\tilde{m}}^{\mathcal{S}}(M)\frac{Z_A}{Z_P^{\mathcal{S}}(M)} \,. \quad (10)$$

As mentioned before, we use the RI′-MOM scheme, [5]. This scheme considers amputated Green's functions (practically in the Landau gauge) with an appropriate operator insertion, here either A or P. The renormalisation point is fixed at some momentum scale $p^2 = \mu_p^2$, and thus we have

$$Z_O^{RI'-MOM}(\mu_p) = \left.\frac{Z_q^{RI'-MOM}(p)}{\frac{1}{12}\mathrm{tr}\left[\Gamma_O(p)\Gamma_{O,BORN}^{-1}(p)\right]}\right|_{p^2=\mu_p^2} , \quad (11)$$

where Γ_O are one-particle irreducible (1PI) vertex functions, and Z_q is the wave-function renormalisation. (Our variation of the implementation of this method is described in [12].) This determines Z_A and $Z_P^{RI'-MOM}$, from which a chiral extrapolation, here using the sea quarks only, may be made to the chiral limit. For Z_A we make a linear extrapolation in am_q, $Z_A = A_A + B_A am_q$, while for $Z_P^{RI'-MOM}$ we must first subtract out a pole in the quark mass, [13], which occurs due to chiral symmetry breaking. We thus make a fit of the form $(Z_P^{RI'-MOM})^{-1} = A_P + B_P/am_q$. We now have all the components, namely A_A, A_P and $\Delta Z_{\tilde{m}}^{RI'-MOM}$ necessary to compute Z_m^{RGI} and hence $r_0 m_q^{RGI}$. In Fig. 3 we show $Z_{\tilde{m}}^{RGI}$ for $\beta = 5.20$, 5.25, 5.29 and 5.40 . These should be independent of the scale $a\mu_p$ at least for larger values. This seems to be the case, we make a phenomenological fit to account for residual effects.

5. COMPARISON OF $Z_{\tilde{m}}^{RGI}$ WITH OTHER METHODS

As many computations of the strange quark mass have used tadpole improved perturbation

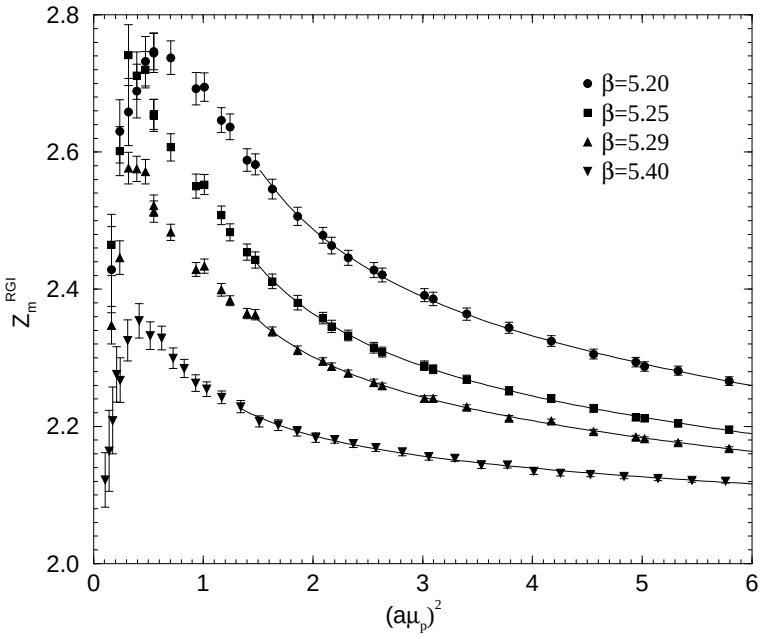

Figure 3. $Z_{\tilde{m}}^{RGI}$ for $\beta = 5.20$ (filled circles), $\beta = 5.25$ (filled squares), $\beta = 5.29$ (filled upper triangles), $\beta = 5.40$ (filled lower triangles) together with fits $F(a\mu_p) = r_1 + r_2(a\mu_p)^2 + r_3/(a\mu_p)^2$.

theory together with a boosted coupling constant for the determination of the renormalisation constant, it is of interest to compare our results obtained in the previous section with this approach. Our variation of this method, tadpole-improved renormalisation-group-improved boosted perturbation theory or TRB-PT, is described in [14]. Regarding the lattice as a 'scheme', then from eq. (2) we can write

$$m_q^{RGI} = \Delta Z_{\tilde{m}}^{LAT}(a)\tilde{m}_q(a)\,, \tag{12}$$

where the renormalisation-group-improved $\Delta Z_{\tilde{m}}^{LAT}(a)$ is given by eq. (3). Furthermore in this 'lattice' scheme, we choose to use $g_{\Box}^2 = g_0^2/u_{0c}^4$ where $u_0^4 = \langle \frac{1}{3}\mathrm{Tr}U^{\Box}\rangle$ ($U^{\Box}$ being the product of links around an elementary plaquette) rather than g_0, as series expansions in $g_{\Box}$ are believed to have better convergence. This is boosted perturbation theory. (We shall use chirally extrapolated plaquette values as determined in [1] at our β-values and so we add a subscript 'c' to u_0.) In the tadpole-improved method, noting that renormalisation constants for operators with no derivatives are $\sim u_{0c}$, which indicates that $Z_{\tilde{m}}^{RGI}u_{0c}^{-1}$ will converge faster then $Z_{\tilde{m}}^{RGI}$ alone we re-write eq. (3) in the two loop approximation as[4]

$$\begin{aligned} Z_{\tilde{m}}^{RGI\,(TRB-PT)} &\equiv \Delta Z_{\tilde{m}}^{LAT}(a) \\ &= u_{0c}\left[2b_0 g_{\Box}^2\right]^{\frac{d_{m0}}{2b_0}}\left[1+\frac{b_1}{b_0}g_{\Box}^2\right]^{q_1}, \end{aligned} \tag{13}$$

where $q_1 = (b_0 d_{\tilde{m}1}^{LAT} - b_1 d_{m0})/(2b_0 b_1) + (p_1/4)(b_0/b_1)$ with $p_1 = \frac{1}{3}$ being the first coefficient in the expansion of u_{0c}. $d_{\tilde{m}1}^{LAT}$ may be found by relating the (known) perturbative result for $Z_{\tilde{m}}^{\overline{MS}}$ to $\Delta Z_{\tilde{m}}^{LAT}$.

In Fig. 4 we plot $Z_{\tilde{m}}^{RGI}$ versus β. Our NP results from section 4 are shown as filled circles. They are to be compared with the TRB-PT results denoted by empty squares. While there is a difference between the results, it is decreasing and thus may be primarily due to remnant $O(a^2)$ effects, which disappear in the continuum limit. That various determinations of $Z_{\tilde{m}}^{RGI}$ have different numerical values can be seen from the results

[4]The TRB-PT subscript in brackets is there only to distinguish the results from those obtained in section 4.

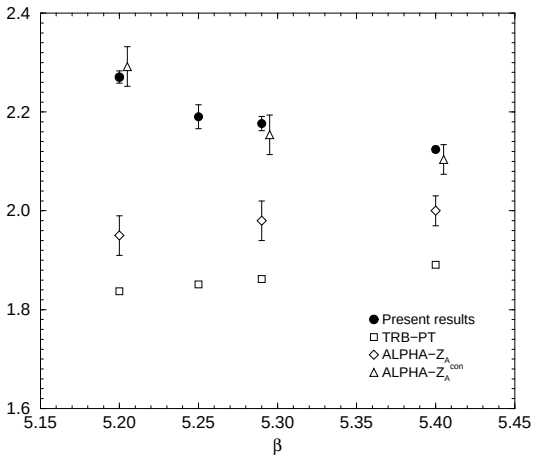

Figure 4. $Z_{\tilde{m}}^{RGI}$ versus β. The black circles are the results from section 4, while the open squares are the TRB-PT results. Furthermore the open diamonds and triangles are the NP results from [11], using the two different results for the axial renormalisation constant, [15]. (The empty triangle results have been slightly displaced for clarity.)

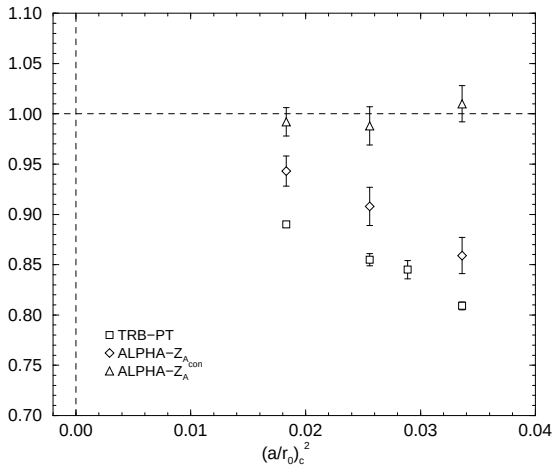

Figure 5. $R_{\tilde{m}}^{X}$ versus $(a/r_0)_c^2$ for X = TRB-PT (open squares), X = ALPHA-Z_A (open diamonds) and X = ALPHA-Z_A^{CON} (open triangles).

of [11] (open diamonds and triangles). In these results two different definitions of the axial renormalisation constant have been used, [15]. Z_A is computed when dropping certain disconnected diagrams, while Z_A^{CON} includes them. (The difference between the two definitions is an $O(a^2)$ effect.) Using Z_A^{CON} in $Z_{\tilde{m}}^{RGI}$ leads, perhaps coincidently, to very similar results to our NP results.

Investigating the possibility of $O(a^2)$ differences a little further, we note that if we have two definitions of $Z_{\tilde{m}}^{RGI}$ then if both are equally valid, forming the ratio should yield

$$R_{\tilde{m}}^{X} \equiv \frac{Z_{\tilde{m}}^{RGI(X)}}{Z_{\tilde{m}}^{RGI}} = 1 + O(a^2)\,, \qquad (14)$$

where $Z_{\tilde{m}}^{RGI}$ is the result of section 4 and X is some alternative definition (i.e. TRB-PT, ALPHA-Z_A, ALPHA-Z_A^{CON}). In Fig. 5 we plot this ratio for these alternative definitions. The r_0/a values used for the x-axis are found by extrapolating the r_0/a results to the chiral limit. This extrapolation and results (for $(r_0/a)_c$) are given in [1].

We see that (roughly) all three ratios extrapolate to 1 which implies that any of the four determinations of $Z_{\tilde{m}}^{RGI}$ may be used. This includes the TRB-PT result. Of course other TI determinations might not have this property, and also their validity always has to be checked against a NP determination, so this result here is of limited use. It is also to be noted that different determinations can have rather different $O(a^2)$ corrections, so a continuum extrapolation is always necessary.

6. RESULTS

Armed with Z_m^{RGI}, we can now find $r_0 m_q^{RGI}$ and hence the ratio $r_0 m_q^{RGI}/(r_0 m_{ps})^2$, using the values of r_0/a given in [7]. In Fig. 6 we plot this ratio (against $(r_0 m_{ps})^2$) for $\beta = 5.29$. Using eq. (4) to eliminate c_a^{RGI} in eq. (5) in favour of $c_{a'}^{RGI}$ where

$$c_{a'}^{RGI} = \frac{r_0 m_s^{RGI}}{(r_0 m_{K^+})^2 + (r_0 m_{K^0})^2 - (r_0 m_{\pi^+})^2}\,, \qquad (15)$$

gives $r_0 m_s^{RGI}$ directly[5] to NLO in our fit function.

We have restricted the quark masses to lie in the range $(r_0 m_{ps})^2 < 5$, which translates to $m_{ps} \lesssim 880\,\mathrm{MeV}$, which is hopefully within the range of validity of low order χPT results. (Using r_0/a, rather than their chirally extrapolated values for example, tends to give less variation in the ratio $r_0 m_q^{RGI}/(r_0 m_{ps})^2$ so we expect LO χPT to be markedly dominant.) Varying this range

[5] This is preferable to first determining c_a^{RGI} and c_i^{RGI}, $i = b, c, d$ by using eq. (5) and then substituting in eq. (4) as the direct fit reduces the final error bar on $r_0 m_s^{RGI}$.

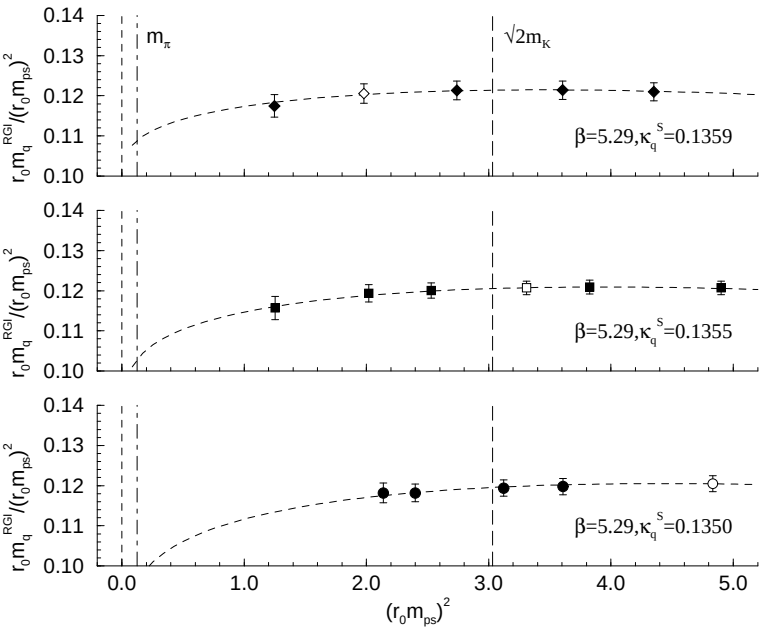

Figure 6. $r_0 m_q^{RGI}/(r_0 m_{ps})^2$ against $(r_0 m_{ps})^2$, together with a fit using eq. (5) for $\beta = 5.29$. Filled points represent valence quark results while unfilled points are the sea quark results. The dashed line (labelled '$\sqrt{2}m_K$') represents a fictitious particle composed of two strange quarks, which at LO χPT is given from eq. (4) by $\sqrt{(r_0 m_{K^+})^2 + (r_0 m_{K^0})^2 - (r_0 m_{\pi^+})^2}$, while the dashed-dotted line (labelled 'm_π') representing a pion with mass degenerate u/d quark is given by $r_0 m_{\pi^+}$.

from 4 to 6 and higher gave some idea of possible systematic errors. Thus finally, for each β-value we have determined $r_0 m_s^{RGI}$ and can now perform the last extrapolation to the continuum limit.

Our derivation so far, although needing a secondary quantity such as r_0/a for a unit, depends only on lattice quantities. Only at the last stage, with our direct fit did we need to give a physical scale to this unit. A popular choice is $r_0 = 0.5\,\text{fm}$. However there are some uncertainties in this value; our derivation using the nucleon gave $r_0 = 0.467\,\text{fm}$ and so to give some idea of scale uncertainties, we shall also consider this value. (The main change when changing the scale comes from the r_0s in eq. (4), as $m_s^{RGI} \propto r_0$, while changes in $\Delta Z_m^{\overline{MS}}$ are only logarithmic.)

Using the value for $[\Delta Z_m^{\overline{MS}}(2\,\text{GeV})]^{-1}$ obtained in section 2 from Fig. 1 to convert m_s^{RGI} to $m_s^{\overline{MS}}(2\,\text{GeV})$ gives the results shown in Fig. 7. Also shown is an extrapolation to continuum limit. We finally obtain the result

$$m_s^{\overline{MS}}(2\,\text{GeV}) = \qquad (16)$$

$$\begin{cases} 117(6)(4)(6)\,\text{MeV} & \text{for} \quad r_0 = 0.5\,\text{fm} \\ 111(6)(4)(6)\,\text{MeV} & \text{for} \quad r_0 = 0.467\,\text{fm} \end{cases} ,$$

where the first error is statistical. The second error is systematic $\sim 3\,\text{MeV}$ estimated by varying the fit interval for $(r_0 m_{ps})^2$. We take a further systematic error on these results as being covered by the different r_0 values of about $\sim 6\,\text{MeV}$. This is to be compared to our previous result using the VWI, [10], which gave results of $126(5)\,\text{MeV}$, $119(5)\,\text{MeV}$ for $r_0 = 0.5\,\text{fm}$ and $0.467\,\text{fm}$ respectively. These results and extrapolation are also shown in Fig. 7.

7. COMPARISONS

It is also useful to compare our results with the results from other groups. In Fig. 8 we show some results for $n_f = 2$ and $n_f = 2 + 1$ flavours (keeping the aspect ratio approximately the same as in Fig. 7. A variety of actions, renormalisations, units and scales have been used (so the results have been plotted in physical units using

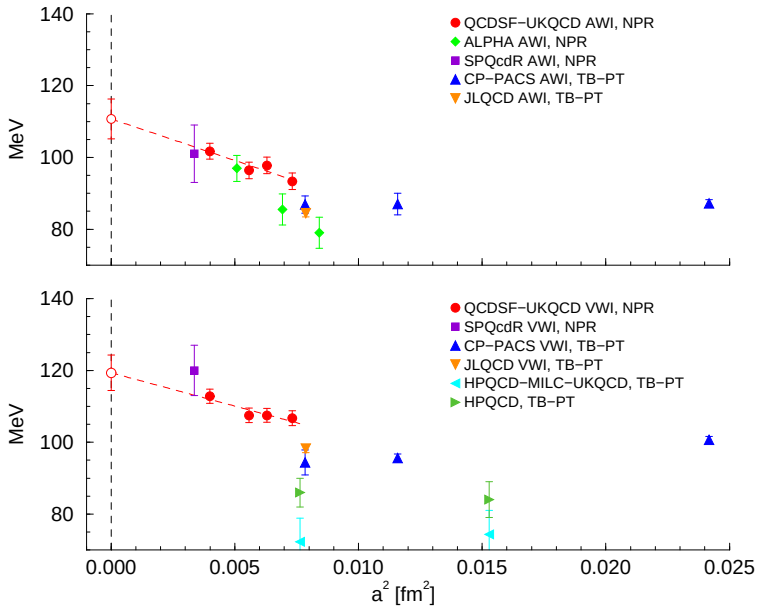

Figure 8. Results for $m_s^{\overline{MS}}(2\,\mathrm{GeV})$ versus $a^2\,\mathrm{fm}^2$ using the AWI (upper plot) and VWI (lower plot) methods. The results are presented with the collaborations preferred units and scales. Circles (together with a linear continuum extrapolation) are from this work and [10]; diamonds from [16]; squares from [17]; up triangles from [18]; down triangles from [19]; left triangles from [20]; right triangles from [21]. NPR denotes non-perturbative renormalisation, while TB-PT denotes tadpole-improved boosted perturbation theory. [20,21] are for $n_f = 2+1$ flavours; the other results are all for $n_f = 2$ flavours.

the authors prefered values). In particular the HPQCD-MILC-UKQCD [21] and HPQCD [20] collaborations use improved staggered fermions. These fermions having a (remnant) chiral symmetry are in the same situation as overlap/domain wall fermions where there is no distinction between VWI and AWI quark masses; the bare quark mass in the Lagrangian simply needs to be renormalised.

As seen earlier in section 5 it is noticeable that the (tadpole improved) perturbative results lie lower than the non-perturbatively renormalised results. Also results with $a \lesssim 0.09\,\mathrm{fm}$ (i.e. $a^2 \lesssim 0.008\,\mathrm{fm}^2$) appear to be reasonably consistent with each other (this is more pronounced for the AWI results than for the VWI results). While results for $a \lesssim 0.09$ show some lattice discretisation effects, using results at larger lattice spacings seems to give a fairly constant extrapolation to the continuum limit. A similar effect has also been seen elsewhere, for example in the determination of $r_0\Lambda^{\overline{MS}}$ for $n_f = 0$ flavours, [7], where coarse lattices also show this characteristic flattening of the data.

Finally, we compare these numbers with results from the QCD sum rule approach. A recent review of results from this method is given in [22], citing as a final result $m_s^{\overline{MS}}(2\,\mathrm{GeV}) = 99(28)\,\mathrm{MeV}$. This covers the lattice results in Fig. 8.

8. CONCLUSIONS

In this article we have estimated the strange quark mass for 2-flavour QCD and found the result in eq. (16), using $O(a)$-improved clover fermions and taking into consideration non-perturbative (NP) renormalisation, the continuum extrapolation of the lattice results and the use of chiral perturbation theory. The NLO chiral perturbation theory yields a correction of about 5% to the LO result, and the relevant low energy constants are in rough agreement with the phenomenological values.

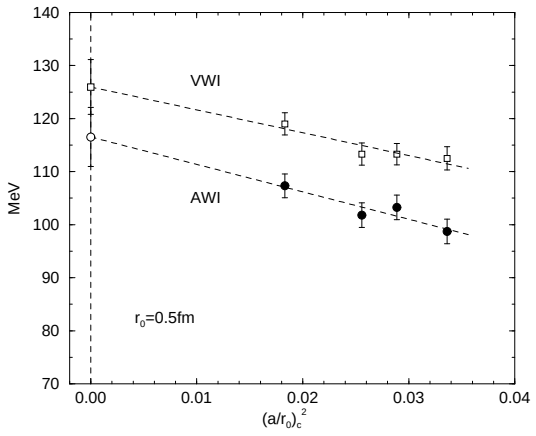

Figure 7. Results for $m_s^{\overline{MS}}(2\,\mathrm{GeV})$ (filled circles) versus the chirally extrapolated values of $(a/r_0)^2$ (as given in [7]) together with a linear extrapolations to the continuum limit. For comparison, we also give our previous result using the VWI, [10] (open squares).

In conclusion, although there is a spread of results, it would seem that the unquenched strange quark mass determined here is not lighter than the quenched strange quark mass and lies in the range of 100 – 130 MeV.

ACKNOWLEDGEMENTS

The numerical calculations have been performed on the Hitachi SR8000 at LRZ (Munich), on the Cray T3E at EPCC (Edinburgh) [23], on the Cray T3E at NIC (Jülich) and ZIB (Berlin), as well as on the APE1000 and Quadrics at DESY (Zeuthen). We thank all institutions. This work has been supported in part by the EU Integrated Infrastructure Initiative Hadron Physics (I3HP) under contract RII3-CT-2004-506078 and by the DFG under contract FOR 465 (Forschergruppe Gitter-Hadronen-Phänomenologie).

REFERENCES

1. QCDSF-UKQCD Collaboration: M. Göckeler et al., hep-lat/0601004.
2. S. Eidelman et al., *Phys. Lett.* B592 (2004) 1.
3. T. van Ritbergen et al., *Phys. Lett.* B400 (1997) 379 [hep-ph/9701390].
4. J. A. M. Vermaseren et al., *Phys. Lett.* B405 (1997) 327 [hep-ph/9703284].
5. G. Martinelli et al., *Nucl. Phys.* B445 (1995) 81 [hep-lat/9411010].
6. K. G. Chetyrkin et al., *Nucl. Phys.* B583 (2000) 3 [hep-ph/9910332].
7. QCDSF-UKQCD Collaboration: M. Göckeler et al., hep-ph/0502212.
8. C. Bernard et al., *Phys. Rev.* D49 (1994) 486 [hep-lat/9306005].
9. S. R. Sharpe, *Phys. Rev.* D56 (1997) 7052, erratum ibid. D62 (2000) 099901 [hep-lat/9707018].
10. QCDSF-UKQCD Collaboration: M. Göckeler et al., hep-ph/0409312.
11. M. Della Morte et al., *JHEP* 0503 (2005) 029 [hep-lat/0503003].
12. QCDSF Collaboration: M. Göckeler et al., *Nucl. Phys.* B544 (1999) 699 [hep-lat/9807044].
13. J. R. Cudell et al., *Phys. Lett.* B454 (1999) 105 [hep-lat/9810058].
14. QCDSF Collaboration: M. Göckeler et al., *Phys. Rev.* D71 (2005) 114511 [hep-ph/0410187].
15. ALPHA Collaboration: M. Della Morte et al., *JHEP* 0507 (2005) 007 [hep-lat/0505026].
16. ALPHA Collaboration: M. Della Morte et al., *Nucl. Phys.* B729 (2005) 117 hep-lat/0507035.
17. SPQcdR Collaboration: D. Bećirević et al., *Nucl. Phys.* B734 (2006) 138 [hep-lat/0510014].
18. CP-PACS Collaboration: A. Ali Khan et al., *Phys. Rev.* D65 (2002) 054505 [Erratum-ibid.D67 (2003) 059901] [hep-lat/0105015].
19. JLQCD Collaboration: S.Aoki et al., *Phys. Rev.* D68 (2003) 054502 [hep-lat/0212039].
20. HPQCD-MILC-UKQCD Collaboration: C. Aubin et al., *Phys. Rev.* D70 (2004) 031504 [hep-lat/0405022].
21. HPQCD Collaboration: Q. Mason et al., hep-ph/0511160.
22. S. Narison, hep-ph/0510108.
23. UKQCD Collaboration: C. R. Allton et al., *Phys. Rev.* D65 (2002) 054502 [hep-lat/0107021].